Nanoscale

MINIREVIEW

View Article Online
View Journal | View Issue

Cite this: *Nanoscale*, 2025, **17**, 6981

External strategies for enhanced sensing performance of self-powered polyvinylidene fluoride-based sensors

Fang Wang, *[a] Zixuan Song,[a] Xinchen Cai,[a] Kai Guo,[a] Xiaoyu Pan,*[c] Chuanlai Ren[d] and Bo Li*[b,d]

Received 10th December 2024,
Accepted 11th February 2025

DOI: 10.1039/d4nr05200e

rsc.li/nanoscale

The era of the Internet of Things has created an increasing demand for self-powered, flexible sensors. Among various intelligent materials, poly(vinylidene fluoride) (PVDF) has emerged as a promising candidate due to its flexibility, processability, biocompatibility, and unique electroactive properties. PVDF's distinctive piezoelectric, pyroelectric and triboelectric characteristics make it particularly suitable for self-powered flexible sensing applications. While research has primarily focused on enhancing the electroactive β phase, PVDF-based sensors still face limitations in their piezoelectric and pyroelectric performance. External strategies such as electrode design, stress/heat transfer improvements, microstructure optimization, and multifunctional synergy show great potential for improving sensing performance. Although numerous reviews address PVDF's polar phase enhancement, there is limited literature overviewing external strategies for performance optimization. This review focuses on external strategies for enhancing the sensing performance of PVDF-based sensors and their emerging applications. It also addresses practical challenges and future directions in PVDF-based sensor development.

1. Introduction

The Internet of Things has brought significant improvements to our lives, particularly through advancements in information collection, analysis, transmission, and storage.[1,2] These developments are poised to revolutionize various areas such as health monitoring, robotic interfaces, and artificial intelligence.[3,4] Among these innovations, flexible multifunctional sensing devices have emerged as a promising technology.[5,6] However, despite the progress made, most sensing systems still rely on batteries, which pose limitations due to their need for frequent recharging or replacement.[6] As a solution, self-powered sensory systems capable of harvesting energy from their environment to power sensors and directly detect external stimuli are receiving increasing attention.[7,8] This has led to growing interest in the development of flexible devices that incorporate piezoelectric, pyroelectric, and triboelectric materials, which can function for both sensing and energy harvesting.[9–13]

Ferroelectric polymers such as poly(vinylidene fluoride) (PVDF) are characterized by mechanical flexibility and possess the best piezoelectric, pyroelectric, and ferroelectric properties among synthetic polymers.[14–16] PVDF is a semicrystalline polymer with five distinct crystalline phases, namely α, β, γ, δ, and ε. Among these, the β, γ, and δ phases are polar, endowing PVDF with piezoelectric, pyroelectric, and ferroelectric properties.[13,16–18] PVDF also exhibits triboelectric behavior due to its high fluorine content and large electronegativity.[19] PVDF finds extensive application in wearable sensors on account of its distinctive electroactive characteristics, flexibility, low-temperature processability, chemical stability, and biocompatibility.[1,20–23] The sensing performance of PVDF is directly associated with its piezoelectric and pyroelectric coefficients, which are influenced by the proportion of the polar phases. Nevertheless, its piezoelectric and pyroelectric capabilities remain inferior to those of inorganic ferroelectric materials. Substantial endeavors have been exerted to enhance the polar phase of PVDF, leading to remarkable advancements in high-performance PVDF-based sensors. Despite this progress, their piezoelectric and pyroelectric performance remains limited and persists as an issue that demands resolu-

[a]*School of Physical Science and Technology, Yangzhou University, Yangzhou 225009, China. E-mail: fang.wang@yzu.edu.cn*
[b]*College of Electrical, Energy and Power Engineering, Yangzhou University, Yangzhou 225009, China. E-mail: bli6@yzu.edu.cn*
[c]*College of Integrated Circuits, Nanjing University of Aeronautics and Astronautics, and Key Laboratory of Aerospace Integrated Circuits and Microsystem, Ministry of Industry and Information Technology, Nanjing 211106, China. E-mail: pxy2024@nuaa.edu.cn*
[d]*Department of Materials Science and Engineering and Guangdong Provincial Key Laboratory of Functional Oxide Materials and Devices, Southern University of Science and Technology, Shenzhen 518055, China*

tion. For instance, the theoretical piezoelectric constant of PVDF is estimated to be 186.3 pC N^{-1} ($|d_{33}|$).[24] The piezoelectric response of a pure polymer can hardly reach 60 pC N^{-1} in actual experiments.[21,25] Consequently, greater endeavors could be directed towards the extrinsic contributions of the sensor structure with the aim of enhancing the sensor's performance.

The sensor's electrode, which collects charges and determines its output properties, plays a critical role in enhancing performance. Key factors such as the contact area and integration of the electrode are crucial for improving sensing capabilities.[26] Additionally, the presence of microstructures can lead to unique electrical properties and cause large deformations under small stresses, which influence the sensor's overall performance.[27] Moreover, with its naturally low elasticity and heat conductivity, PVDF, requires efficient stress and heat transfer from the surface to the inner material or fillers to enhance the response of internal dipoles to external stimuli.[13,28–30] In addition to its piezoelectric and pyroelectric properties, PVDF exhibits triboelectric behavior due to its high fluorine content and substantial electronegativity.[19] The synergistic effects of piezoelectric, pyroelectric, and triboelectric properties can further enhance the sensing performance of PVDF-based materials.[31] These strategies focus not only on the internal polar phase of PVDF but also on external factors that influence sensor output. Although numerous reviews discuss improvements to PVDF's polar phase,[15,32–34] there remains a gap in the literature concerning external strategies to enhance its sensing performance.

This paper is dedicated to presenting an overview of the recent advancements in PVDF-based sensors, with a particular emphasis on enhancing sensing performance through extrinsic strategies and their corresponding applications. From a fundamental perspective, we discuss the principal factors affecting the sensing capabilities of PVDF-based sensors. Additionally, we highlight diverse external strategies including electrode design, stress/heat transfer improvements, microstructure optimization, and multifunctional synergy (Fig. 1), along with their applications in health monitoring, robotic interfaces, and artificial intelligence. Finally, we also deliberate on the challenges that PVDF-based sensors currently face and provide valuable insights into the prospective directions for their further development.

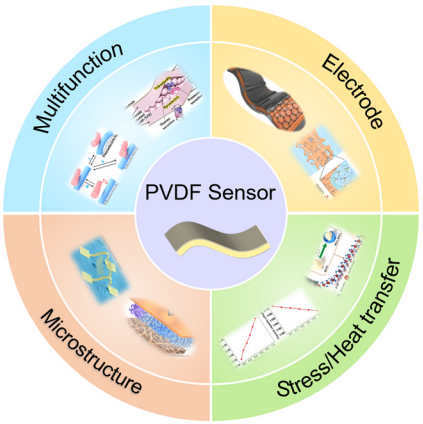

Fig. 1 External strategies to enhance sensing performance of poly(vinylidene fluoride)-based sensors include electrode design, stress/heat transfer improvements, microstructure optimization, and multifunctional synergy. Reproduced with permission.[35] Copyright 2014, Wiley-VCH. Reproduced with permission.[26] Copyright 2023, Springer Nature. Reproduced with permission.[36] Copyright 2020, Elsevier Ltd. Reproduced with permission.[28] Copyright 2023, Wiley-VCH. Reproduced with permission.[37] Copyright 2025, Wiley-VCH. Reproduced with permission.[38] Copyright 2019, Springer Nature. Reproduced with permission.[39] Copyright 2024, American Chemical Society. Reproduced with permission.[40] Copyright 2022, Wiley-VCH.

2. The principles of PVDF-based sensors

The direct piezoelectric effect refers to the ability of certain materials with asymmetric crystal structures to generate an electrical potential when subjected to pressure or force. The pyroelectric effect, on the other hand, involves a change in spontaneous polarization in certain polar materials due to temperature fluctuations. Mostly, the direct piezoelectric and pyroelectric effects of PVDF are employed by the sensors. A typical PVDF-based sensor consists of a PVDF layer sandwiched between two electrodes. When a mechanical stress ($\Delta\sigma$) or temperature fluctuation (ΔT) is applied to the sensor, the open circuit voltage (V_{oc}) and the short-circuit current (I_{sc}) for the PVDF-based sensor can be obtained[41]

$$V_{oc} = \frac{d_{33}}{\varepsilon_{33}} h\Delta\sigma \text{ or } V_{oc} = \frac{p}{\varepsilon_{33}} h\Delta T \quad (1)$$

$$I_{sc} = d_{33} A \mathrm{d}\sigma/\mathrm{d}t \text{ or } I_{sc} = pA\mathrm{d}T/\mathrm{d}t \quad (2)$$

where d_{33}, ε_{33}, h, p, A, $\mathrm{d}\sigma/\mathrm{d}t$, $\mathrm{d}T/\mathrm{d}t$ are the piezoelectric coefficient, permittivity, thickness of PVDF layer, pyroelectric coeffi-

Fang Wang

Fang Wang is currently an Associate Professor at Yangzhou University. She received her Ph.D. in 2014 from the Xiangtan University, and worked as a postdoctoral researcher at Shenzhen Institute of Advanced Technology (SIAT), Chinese Academy of Sciences (CAS) in 2019. Her research interests include developing ferroelectric materials, approaches, and technologies for sensors, energy harvesting, object manipulation, and neural stimulation. She has published over 30 peer-reviewed papers in reputed international journals, including Science Advances, National Science Review and The Innovation.

cient, effective area of the sensor, the rate of mechanical stress change and the rate of temperature change, respectively.

Additionally, PVDF is widely used as a negative material in triboelectric sensors. Its large dipole moment, high flexibility, excellent formability, strong electronegativity, and outstanding dielectric properties make PVDF and its copolymers highly promising materials in this field.[7,42,43]

The performance of a sensor can be evaluated using various parameters, including sensitivity, durability, and response/recovery kinetics. Among these, sensitivity is a key factor, defined as the ratio of the sensor's response to the corresponding input. In some cases, sensitivity for force or temperature detection through piezoelectric or pyroelectric sensors can be calculated using the following equation[44,45]

$$S = V_{oc}/\Delta\sigma \text{ or } S = I_{sc}/\Delta\sigma \quad (3)$$

$$S = V_{oc}/\Delta T \text{ or } S = I_{sc}/\Delta T \quad (4)$$

To maximize sensitivity, high values of d_{33}, p, $d\sigma/dt$, and dT/dt are essential. In addition to the intrinsic contributions of the PVDF's polar phase to d_{33} and p, extrinsic factors, such as a large electrode area and a high rate of stress and temperature change, play a crucial role in enhancing the sensitivity.[30] Therefore, strategies about the piezoelectric and pyroelectric sensors structure used to enhance the charge accumulation and polarization change rate are considerable. For triboelectric sensors, the sensing performance depends not only on the device geometry but also on the properties of the materials used in pairing. Key factors include the dielectric properties, surface charge density, effective frictional contact area, and surface chemical characteristics of the materials.[19,46–48]

3. External strategies for enhanced sensing performance

External strategies aimed at enhancing the charge accumulation and polarization change rate are critical for achieving high sensing performance in PVDF-based sensors. This section summarizes external strategies for enhancing sensing performance, including electrode design, stress/heat transfer improvements, microstructure optimization, and multifunctional synergy.

3.1. Electrode

Electrodes act as charge accumulators, collecting the sensor's charge changes during stimulation and directly generating an electric signal.[49,50] Traditionally, metal foil electrodes were either physically placed or metal-coated thin film electrodes were applied to the top and bottom surfaces of PVDF-based layers.[51] However, poor adhesion between metal electrodes and the hydrophobic PVDF surface could cause electrode detachment. To improve adhesion, ion beam and/or plasma treatments were used to modify the surface energy,[52] or medium layers were added.[53] While these methods significantly enhanced interfacial adhesion, the brittleness of metal electrodes resulted in poor fatigue resistance, leading to electrode failure. Mismatches in Young's modulus and Poisson's ratio between the metal electrodes and PVDF-based layers destabilized the structure due to interfacial shear stress.

To address the mechanical mismatch between electrodes and PVDF-based materials, flexible fiber-structured metal electrodes or organic conductive electrodes were explored.[54,55] For example, a micro-patterned polydimethylsiloxane (PDMS)–carbon nanotube (CNT) composite was used as the top electrode, while graphene nanosheets served as the bottom electrode for P(VDF–TrFE) materials. The use of flexible electrodes effectively resolved the mechanical mismatch between the electrodes and PVDF-based materials, offering significantly improved robustness and stability in sensor performance compared to conventional metal electrodes.[35] Furthermore, these flexible electrodes deform in sync with the PVDF-based materials, facilitating efficient electron collection during deformation and thereby enhancing the output performance of the piezoelectric sensor. To further improve the adhesion between the electrodes and the matrix, Maity *et al.* employed vapor-phase polymerization to deposit the organic conductive polymer poly(3,4-ethylenedioxythiophene) (PEDOT) onto the surfaces of PVDF nanofibers, creating a multilayer networked structure that integrated compatible electrodes. This structure demonstrated exceptional sensitivity to human movements, such as foot strikes and walking. Notably, continuous fatigue tests over six months underscored its potential as a durable wearable mechanical energy harvester and sensor.[56]

Moreover, Simaite and colleagues employed a combination of chemical chain entanglement and mechanical interlocking to achieve strong adhesion between poly(3,4-ethylenedioxythiophene) poly(styrenesulfonate) (PEDOT:PSS) and PVDF. They utilized argon-plasma-induced surface polymerization of poly (ethylene glycol) monomethyl ether methacrylate (PEGMA), resulting in hydrophilic PVDF-*graft*-PEGMA outer surfaces and a hydrophobic bulk core. Subsequently, a PEDOT:PSS aqueous solution was used to fill the pores of the functionalized portion of the membrane, creating a penetrated interlayer between the PEDOT:PSS and PVDF (Fig. 2c). These structures exhibited strains of 0.6% and showed no signs of delamination after over 150 hours or 10^4 actuation cycles.[57] The penetrated electrode not only enhances adhesion but also expands the area for charge collection. Researchers found that penetrated electrodes, forming a nanoscale-conducting network on fiber surfaces, improved interactions between electrodes and PVDF nanofibers. This enlarged contact area and increased conductive pathways enhanced piezoelectric signals and energy conversion efficiency, strengthening the overall sensitivity.[58] Li *et al.* improved charge collection in a poly(vinylidene fluoride-*co*-trifluoroethylene) (P(VDF–TrFE)) thin film by cross-linking it with a PEDOT:PSS layer (Fig. 2d). The resulting P(VDF–TrFE)/PEDOT:PSS composite film exhibited an ultrasensitive and linear mechanical/thermal response, with sensitivities of 2.2 V kPa^{-1} in the pressure range of 0.025–100 kPa and 6.4 V K^{-1} in the temperature range of 0.05–10 K. The enhanced charge collection, resulting from the interface network

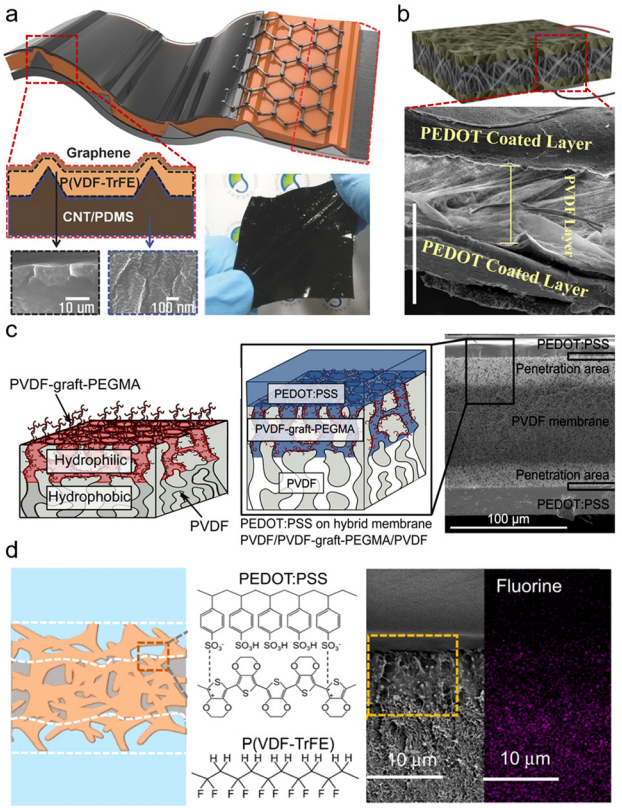

Fig. 2 Electrode designs for high-performance PVDF-based sensors. (a) CNT/PDMS composite and graphene nanosheets used as top and bottom electrodes for P(VDF–TrFE) material. Reproduced with permission.[35] Copyright 2014, Wiley-VCH. (b) Multilayer-assembled electrospun PVDF nanofiber mats with vapor-phase polymerized PEDOT-coated PVDF nanofibers as electrodes. Reproduced with permission.[56] Copyright 2018, American Chemical Society. (c) PEDOT:PSS/PVDF-*graft*-PEGMA/PEDOT:PSS actuators with strong adhesion between electrodes and PVDF. Reproduced with permission.[57] Copyright 2015, American Chemical Society. (d) Network interconnection interface of P(VDF–TrFE)/PEDOT:PSS composite film. Reproduced with permission.[26] Copyright 2023, Springer Nature.

between PEDOT:PSS and P(VDF–TrFE), led to a piezoelectric coefficient of −86 pC N^{-1} and a pyroelectric coefficient of 95 μC m^{-2} K^{-1}. This demonstrates how electrode interface engineering can boost the sensitivity of ferroelectric polymer sensors.[26]

In conclusion, electrodes play a vital role in charge collection, adhesion, and adaptability. An effective contact area significantly improves the sensitivity and durability of PVDF sensors.

3.2. Stress/heat transfer

PVDF inherently exhibits low elasticity and thermal conductivity.[59,60] Therefore, efficient transfer of stress and heat from the surface to the internal material or fillers is essential for enhancing the response of internal dipoles to external stress or thermal stimuli.[30,61–66] Typically, fillers with high elasticity or thermal conductivity are incorporated into PVDF-based materials to improve stress and heat transfer.

Shi *et al.* grafted a layer of high-modulus polymethyl methacrylate (PMMA) onto the surface of $BaTiO_3$ (BTO) nanowires *via* surface-initiated polymerization. The high elasticity coating can improve the dispersion of the nanowires and enhancing stress transfer at the interface. This resulted in improved output performance in the fibrous nanocomposite piezoelectric nanogenerators.[67] Li *et al.* designed a polymer–nanoparticle–liquid ternary composite consisting of polydopamine-modified barium titanate nanoparticles (PDA–BTO NPs), polyvinylidene fluoride (PVDF), and 1*H*,1*H*,2*H*,2*H*-perfluorodecyltriethoxysilane (PFOES) liquid nanodroplets. The PFOES nanodroplets formed a 3D scaffold matrix within the composite. Finite element analysis showed that the ternary composite had significantly improved stress transfer capability due to the highly deformable PFOES liquid nanodroplets, which increased the net stress exerted on the PDA–BTO NPs and the PVDF matrix (Fig. 3a). This composite exhibited enhanced piezoelectric performance, achieving an output voltage of 102 V, a current of 10 μA, and a power density of 70 μW cm^{-2}, which were record-high values compared to binary composite-based devices. Furthermore, the device showed great potential as a highly sensitive tactile perception tool for shape recognition.[68] In addition to the high elasticity of the fillers, their alignment is crucial for effective stress transfer. A 3D printing technique was employed to achieve *in situ* dipole alignment of PVDF within PVDF-2D molybdenum disulfide (2D MoS_2). During the 3D printing process, shear stress-induced dipole poling of PVDF and alignment of 2D MoS_2 are leveraged to enhance piezoelectricity, eliminating the need for a post-poling process. The strain transfer to the nanofillers was confirmed through microstructural analysis and finite element simulations (Fig. 3b).[69]

As thermal conductivity is crucial for heat transfer, increasing it in pyroelectric materials improves the rate of temperature change (dT/dt). High thermal conductivity fillers, such as diamond, beryllia, aluminum nitride, aluminum oxide,[30] and liquid metals,[70–72] are commonly incorporated into thermally insulating matrices to create a conductive network that enhances phonon transportation and heat transfer.[30] Li *et al.* improved the pyroelectric properties of P(VDF–TrFE) films by incorporating inorganic P-type bismuth antimonide (P-Bi_2Te_3) fillers. Composite films with 0.2 wt% P-Bi_2Te_3 showed improved pyroelectric response time and voltage due to increased thermal diffusivity and enhanced β-phase content. Proton irradiation further reduced the pyroelectric response time from 22 to 0.5 s due to the ionization energy loss from proton irradiation enhanced the conductivity of the composite film (Fig. 3c).[28] Additionally, an interpenetrating structure of poly(vinylidene fluoride–trifluoroethylene–chlorofluoroethylene) (P(VDF–TrFE–CFE)) polymer and ceramic materials with highly conductive pathways was developed, achieving a 300% increase in thermal conductivity (Fig. 3d). The continuous 3D thermal conductive network facilitated rapid phonon conduction, addressing the challenge of slow heat dissipation in

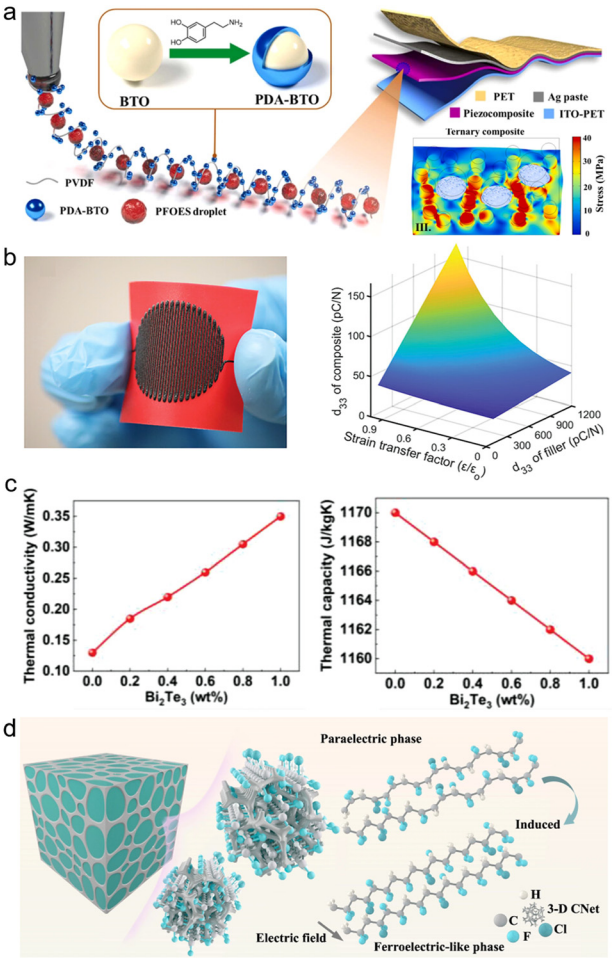

Fig. 3 Stress/heat transfer improvements for high performance PVDF-based sensor. (a) PFOES nanodroplets enable the formation of a three-dimensional scaffold matrix in the PDA–BTO nanoparticle-doped PVDF composite, enhancing stress transfer. Reproduced with permission.[36] Copyright 2020, Elsevier Ltd. (b) 3D printing PVDF–MoS_2 composite with boosting piezoelectricity. Reproduced with permission.[69] Copyright 2023, Wiley-VCH. (c) P-Bi_2Te_3/P(VDF–TrFE) composite films improve thermal diffusivity. Reproduced with permission.[28] Copyright 2023, Wiley-VCH. (d) The continuous 3D thermally conductive networks of ferroelectric polymer/ceramic composite. Reproduced with permission.[73] Copyright 2022, Springer Nature.

PVDF-based polymers and their contact interfaces with low thermal conductivity.[73]

Therefore, the utilization of high elasticity or thermal conductivity fillers can significantly enhance the stress/heat transfer capabilities of PVDF-based sensors. However, it is essential to take into account the effective interface between the fillers and PVDF. There is a demand for well-designed interfaces or structures.

3.3. Microstructure

The microstructure plays a significant role in influencing the electrical properties of PVDF-based sensors. This is due to the increased specific surface area, which promotes a stronger strain response, stress concentration, and enhanced stress transfer. These factors collectively contribute to an improvement in the triboelectric properties, thereby affecting the sensing performance of the sensors.[27] One widely used microstructure is the porous structure, which can be easily fabricated.[27,74] PVDF-based layer with porous structures is inclined to deformation and stress concentration due to the presence of internal pores. Moreover, the porous structure, owing to its larger specific surface area and strong strain response, is beneficial for attaining a high electromechanical coupling factor. Additionally, certain porous materials exhibit a reduced Young's modulus and enhanced stress transfer. Collectively, these aspects enable PVDF-based porous sensors to possess a greater piezoelectric output and enhanced sensitivity.[27,75] Lee *et al.* demonstrated that electrospun P(VDF–TrFE) fibers with higher surface porosity outperform their smooth-surfaced counterparts in terms of output voltage and power generation. Theoretical and numerical studies support the benefit of structural porosity, linking it to local stress concentration and a reduced dielectric constant due to air in the pores (Fig. 4a).[76] A porous structure was fabricated using a novel optimized quenching method to create a PVDF and PMMA porous blend (Fig. 4b). The triboelectric nanogenerators (TENGs) exhibit exceptional electrical output, featuring a dielectric constant of 40 and an open-circuit voltage of approximately 600 V. The porous matrix significantly enhances durability, maintaining stable performance over 36 000 operational cycles without degradation.[37]

To further refine microstructure design, PVDF-based materials with micro-pyramids,[70,71,77] micropillars,[78–82] hemispherical,[83] and biomimetic structures[40,84,85] have been developed. These microstructures exhibit large deformations under small stress, and large stress concentration around the special geometries, which causes significant changes in dipole density, making them ideal for detecting weak mechanical excitation. For example, P(VDF–TrFE) films with micro-pyramid structures generate nearly five times more power output than flat films, exhibiting an ultrasensitive response to mechanical deformation.[77] Hierarchical structures, which integrate specific design elements to optimize overall performance, have also been explored.[86] PVDF-based sensors with hierarchical structures show greater potential for superior electrical output, detection sensitivity, and durability due to the complex mechanical and electrical coupling effects. Yang *et al.* developed a 3D hierarchically interlocked PVDF/ZnO nanofiber-based piezoelectric sensor by epitaxially growing ZnO nanorods on electrospun PVDF nanofiber. The ZnO nanorods' hierarchical structure enabled significant deformation, resulting in a stronger piezoelectric potential. The sensor exhibited a substantial increase in sensitivity—6 times greater in pressing mode and 41 times greater in bending mode compared to pure PVDF nanofibers (Fig. 4c).[87]

To address the limited stretchability of PVDF due to its plastic nature, complex microstructures have been designed.[75] A 3D buckled structure, composed of a serpentine PVDF ribbon and a proof mass (Cu, 500 μm × 500 μm × 500 μm), gen-

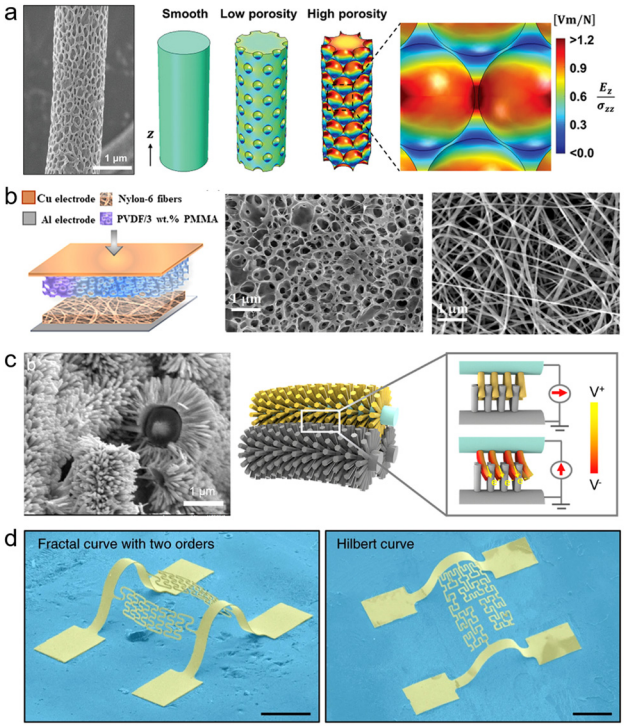

Fig. 4 Microstructure optimization for high performance PVDF-based sensor. (a) The fabrication and structure of P(VDF–TrFE) fibers with surface porosity. Reproduced with permission.[76] Copyright 2022, Wiley-VCH. (b) TENG fabricated by PVDF and PMMA porous blend. Reproduced with permission.[37] Copyright 2025, Wiley-VCH. (c) Hierarchically structured PVDF/ZnO core–shell nanofibers. Reproduced with permission.[87] Copyright 2020, Elsevier Ltd. (d) 3D buckled structure with a serpentine PVDF ribbon with ultralow stiffness. Reproduced with permission.[38] Copyright 2019, Springer Nature.

erates electrical power across frequencies from 5 Hz to 500 Hz under out-of-plane vibrations with accelerations ranging from 4 g to 0. The 3D buckled serpentine structure shows ultralow-stiffness and asymmetric designs, generates significantly larger output voltage than a 2D serpentine across a broad frequency range (Fig. 4d).[38]

3.4. Multifunctional synergy

In addition to possessing piezoelectric and pyroelectric properties simultaneously, PVDF also exhibits triboelectric behavior due to its high fluorine content and large electronegativity.[19] The combination of piezoelectric, pyroelectric, and triboelectric effects enables to enhance the sensing performance of PVDF-based materials.[31,35,36,39,88–91]

Both piezoelectric and triboelectric processes can occur under pressure. Consequently, the simultaneous occurrence of both piezoelectric and triboelectric conversion may enhance the electrical signal. Huang *et al.* demonstrated a monolayer membrane created by co-electrospinning binary fiber nanocomposites, incorporating multiwalled carbon nanotubes (CNTs) into PVDF and polyacrylonitrile (PAN). The resulting PVDF/CNT$_X$@PAN/CNT$_X$ membrane exhibited an outstanding synergistic effect between piezoelectricity and triboelectricity, along with high machine-to-electric conversion efficiency (Fig. 5a). This piezoelectric nanogenerator delivered excellent electrical output (187 V and 8.0 μA), which was 5.1 and 4.6 times higher than that of PAN or PVDF single-fiber membranes, respectively. The sensor accurately detected human movement, ranging from small to large motions, and demonstrated potential applications in medical, firefighting, and monitoring systems.[39] The polarization direction of PVDF influences its triboelectric properties, likely due to the induction driven by piezoelectric charges.[19] Šutka *et al.* demonstrated a novel piezoelectric–electrostatic generator constructed from inversely polarized PVDF films, which exhibits superior performance compared to TENGs in converting mechanical energy to electricity (Fig. 5b).[92]

Shin *et al.* reported the combination of triboelectric and pyroelectric effects in inversely polarized P(VDF–TrFE) pairs. They developed a self-powered multimodal pressure-temperature sensor utilizing a single P(VDF–TrFE) material, which switches the triboelectric polarity through ferroelectric polarization (Fig. 5c). The inversely-polarized P(VDF–TrFE) device showed ~106 times and ~12 times higher triboelectric and pyroelectric currents, respectively, compared to non-polarized devices. This device achieved a high-pressure sensitivity of 40 nA kPa^{-1} and 1.4 V kPa^{-1} over a broad pressure detection range (98 Pa–98 kPa) and competitive temperature sensitivity of 0.38 nA °C^{-1} and 0.27 nA °C^{-1} in cooling and heating states. As a result, it can differentiate multiple stimuli, including pressure and temperature, without signal interference.[36] Additionally, a self-powered flexible antibacterial tactile sensor was developed, utilizing a triboelectric–piezoelectric–pyroelectric multi-effect coupling mechanism. This mechanism analyzes the coupled bimodal voltage signal with response time differences to differentiate external stimuli. This sensor allows multifunctional sensing in a single pixel, reducing structural complexity. The sensor showed pressure sensitivity of 0.092 V kPa^{-1} and temperature sensitivity of 0.11 V °C^{-1}.[31]

4. Applications

External strategies, combined with internal polar phase enhancements, have contributed to the development of high-performance sensors. For instance, the design of flexible and penetrative electrodes improves the adhesion between the electrode and matrix, making the sensor more suitable for complex deformation applications. Furthermore, advancements in stress and heat transfer mechanisms significantly enhance output performance, particularly for high-sensitivity applications. Microstructure optimization also increases the sensor's flexibility and sensitivity, while multifunctional synergies further improve output performance, enabling simultaneous detection of multiple signals. As a result, PVDF-based self-powered flexible sensors offer broad applications across various fields, including health monitoring, robotic interfaces,

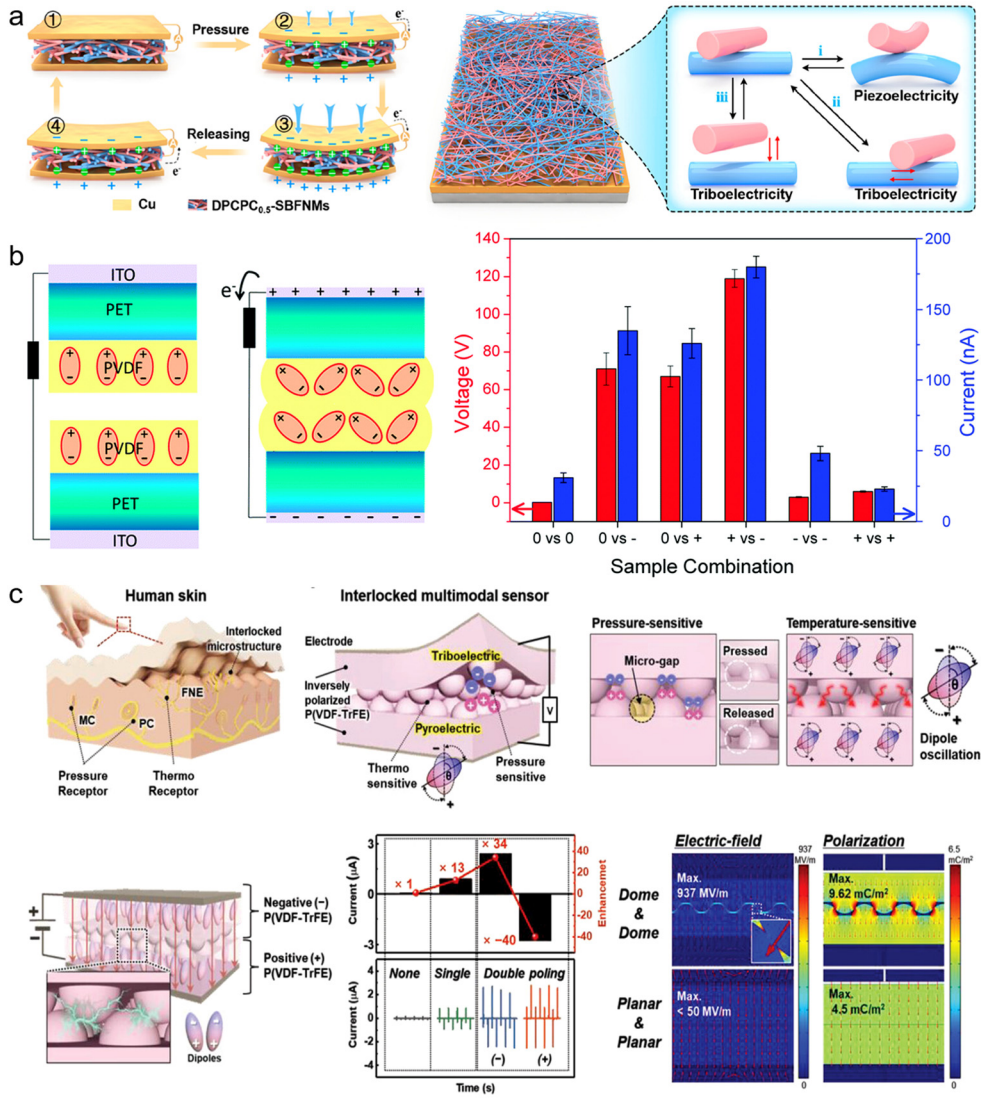

Fig. 5 Multifunctional synergy for high performance PVDF-based sensor. (a) A multifunctional nanogenerator and self-powered sensor system based on PVDF/CNT$_X$@PAN/CNT$_X$ interpenetrating nanocomposite fibers, combining piezoelectric and triboelectric effects. Reproduced with permission.[39] Copyright 2024, American Chemical Society. (b) Inversely polarized PVDF films enhance the output performance of TENGs. Reproduced with permission.[92] Copyright 2018, Royal Society of Chemistry. (c) Skin-inspired ultrasensitive multimodal sensors using inversely polarized P(VDF–TrFE) with an interlocked microstructure for pressure and temperature sensing. Reproduced with permission.[40] Copyright 2022, Wiley-VCH.

and artificial intelligence, with notable advantages such as high sensitivity, durability, and rapid responsiveness.[46,93–96]

Wearable sensors enable non-invasive monitoring of various human physical and physiological parameters, playing an increasingly crucial role in the healthcare system, especially with the rapid advancement and widespread application of information technology.[97–100] These sensors must be flexible enough to conform to the complex contours of the body and possess high sensitivity to detect subtle physiological changes.[101] In health monitoring applications, hierarchically structured PVDF/ZnO core–shell nanofibers, known for their excellent flexibility and high sensitivity in both pressing and bending modes, have been developed. Leveraging these properties, the sensor can accurately detect subtle physiological signals such as respiration, wrist pulse, and muscle activity. Additionally, a highly sensitive gait recognition system was successfully implemented using sensor arrays (Fig. 6a).[87]

Human–machine interaction, the communication between humans and machines *via* user interfaces, is garnering increasing attention due to its wide range of applications in fields such as robotic manipulation, smart prosthetics, and entertainment.[102–106] Smart piezoelectric and pyroelectric sensors are emerging as key components for human–machine interaction, offering essential capabilities for information interaction.[107–109] PVDF-based sensors perform exceptionally well in critical areas like sensitivity, stretchability, resolution, stability, biocompatibility, and miniaturization. A microstructure optimization 3D geometry PVDF design that increases the

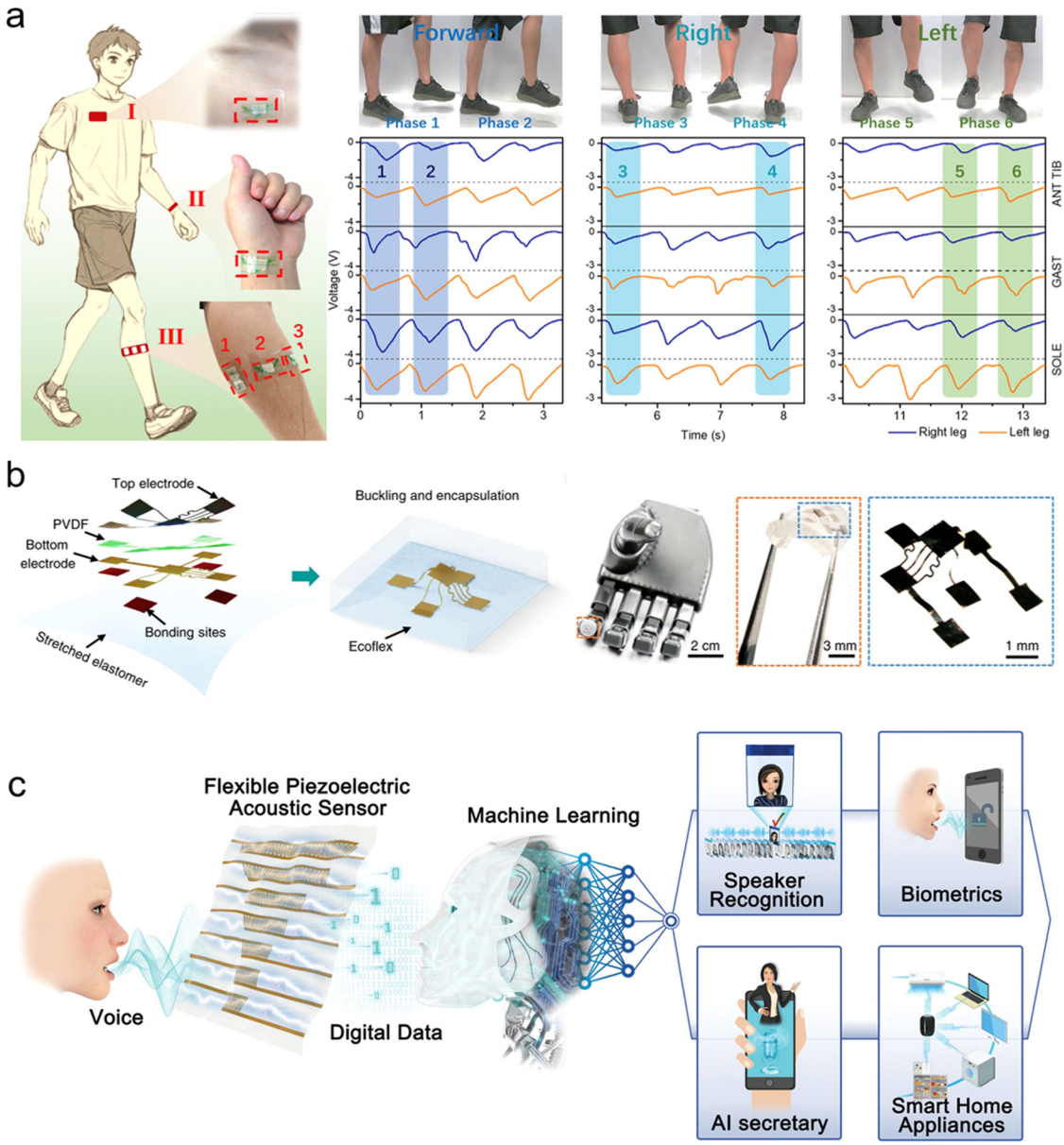

Fig. 6 Applications of PVDF-based sensors. (a) Hierarchically interlocked PVDF/ZnO nanofiber-based piezoelectric sensor detects subtle physiological signals. Reproduced with permission.[87] Copyright 2020, Elsevier Ltd. (b) Three-dimensional piezoelectric polymer microsystems for robotic interfaces. Reproduced with permission.[38] Copyright 2019, Springer Nature. (c) Flexible piezoelectric acoustic sensors for machine learning. Reproduced with permission.[113] Copyright 2020, Wiley-VCH.

number of deformation degrees of freedom, creating new possibilities for robotic interface design. By encapsulating these 3D structures in soft silicone elastomers, the device is physically protected while maintaining its flexibility (Fig. 6b). These advancements in mechanical sensing open up potential pathways for the development of robotic prosthetic interfaces. Additionally, integrating multiple devices over a large area in a distributed manner allows for gesture recognition, spatiotemporal mapping of motions, and other applications[38] (Fig. 6c).

In the field of artificial intelligence, piezoelectric sensors are gaining attention for their use in flexible acoustic sensors for speech recognition and artificial synapses.[110–112] Piezoelectric acoustic sensors, with their excellent inherent properties, are promising candidates to enhance sensitivity and improve speech recognition accuracy. As shown in Fig. 6c, a speech recognition system typically consists of two essential components: (i) acoustic hardware sensors, and (ii) speech recognition software. The acoustic sensors detect the sound pressure of human speech and convert it into analog electrical signals. These sensors capture the vibrations caused by speech, providing vast amounts of data for preprocessing and model training.[113] A key challenge for PVDF-based sensors in

artificial intelligence applications remains their relatively low sensitivity. However, ongoing improvements to these PVDF-based sensors through external strategies hold significant promise for enhancing their performance and expanding their potential use in artificial intelligence.

PVDF-based flexible sensors have emerged as versatile and highly sensitive devices with applications in health monitoring, robotic interfaces, and artificial intelligence. These sensors possess the capacity to foster the establishment of more personalized and continuous monitoring systems, as well as more seamless and intuitive interactions between humans and machines. Thereby, they contribute to the earlier disease detection and more effective treatment, to the augmentation of the functional capabilities of prosthetics and open up new frontiers in intelligent sensing and interaction technologies.

5. Summary and outlook

Over the past decade, PVDF-based sensors have been extensively explored, developed, and applied in various fields. In this review, recent advances in PVDF-based sensors aimed at improving sensing performance through external strategies and their applications are summarized and discussed. These advances include the main factors affecting the sensing performance of PVDF-based sensors and highlight diverse strategies, including electrode design, stress/heat transfer optimization, microstructural modifications, and multifunctional synergy, as well as their applications in health monitoring, robotic interfaces, and artificial intelligence. Despite the progress made through external strategies to improve PVDF-based sensors, many challenges and opportunities remain that need to be addressed in order to realize practical applications in the era of the Internet of Things.

While significant efforts have been made to improve the sensing performance of PVDF-based sensors, further advancements are still required to enhance their piezoelectric, pyroelectric, and triboelectric responses. In terms of electrode design, flexible and penetrative electrodes have notably improved adhesion and contact area with PVDF. However, methods that can simultaneously achieve high polar phase alignment and effective electrode penetration remain scarce. The use of porous structures or nanofibers, which are conducive to surface functionalization and electrode penetration, often fails to achieve high polar phase alignment along the *z*-direction. Consequently, the development of more effective preparation techniques is essential. Regarding stress and heat transfer improvements, the primary challenge lies in the interface between the filler and PVDF. To achieve significant changes in elastic or thermal conductivity, a large amount of filler material is required, which can lead to agglomeration that deteriorates both electrical and mechanical properties. Thus, resolving the issue of interfacial compatibility is crucial. Microstructure optimization, particularly through the integration of electrode design and stress/heat transfer improvements, holds promise for further enhancing the sensing performance of PVDF-based sensors. In terms of multifunctional synergy, there is a need for piezoelectric enhancement of the triboelectric effect. Additionally, the issue of crosstalk between output signals, especially those from the piezoelectric and triboelectric effects, needs to be addressed. Decoupling these output signals to enable accurate detection of each stimulus is of paramount importance.

Both external and internal strategies to enhance the polar phase of PVDF can work synergistically to boost sensor performance. Moreover, achieving a balance between the mechanical and electrical properties of PVDF is still a significant challenge.[29] For instance, the addition of fillers to enhance electrical properties may compromise the material's flexibility, which is critical for applications requiring adaptation to curved surfaces. Furthermore, the durability and fatigue resistance of PVDF-based sensors directly influence signal integrity and determine their lifespan in real-world applications. Strategies that optimize the mechanical compatibility, affinity, and conductivity of electrodes offer promising solutions to enhance the durability and practical applicability of these sensors.

Data availability

This is a review article. The data presented in this review were obtained from the cited references. The original data sources can be accessed by following the citations provided in the text. No additional data was generated or collected for this review.

Conflicts of interest

The authors declare no conflict of interest.

Acknowledgements

The authors acknowledge the financial support provided by the Guangdong Basic and Applied Basic Research Foundation (2023A1515012638).

References

1 B. Stadlober, M. Zirkl and M. Irimia-Vladu, *Chem. Soc. Rev.*, 2019, **48**, 1787–1825.
2 S. T. Han, H. Y. Peng, Q. J. Sun, S. Venkatesh, K. S. Chung, S. C. Lau, Y. Zhou and V. A. L. Roy, *Adv. Mater.*, 2017, **29**, 1700375.
3 W. Deng, Y. Zhou, A. Libanori, G. Chen, W. Yang and J. Chen, *Chem. Soc. Rev.*, 2022, **51**, 3380–3435.
4 J. D. Shi, S. Liu, L. S. Zhang, B. Yang, L. Shu, Y. Yang, M. Ren, Y. Wang, J. W. Chen, W. Chen, Y. Choi and X. M. Tao, *Adv. Mater.*, 2020, **32**, 1901958.
5 Y. Khan, A. E. Ostfeld, C. M. Lochner, A. Pierre and A. C. Arias, *Adv. Mater.*, 2016, **28**, 4373–4395.

6 B. H. Wang and A. Facchetti, *Adv. Mater.*, 2019, **31**, 1901408.
7 F. R. Fan, W. Tang and Z. L. Wang, *Adv. Mater.*, 2016, **28**, 4283–4305.
8 R. Y. Liu, Z. L. Wang, K. Fukuda and T. Someya, *Nat. Rev. Mater.*, 2022, **7**, 870–886.
9 X. Yuan, J. Shi, Y. Kang, J. Dong, Z. Pei and X. Ji, *Adv. Mater.*, 2024, **36**, 2308726.
10 X. Pu, C. Zhang and Z. L. Wang, *Natl. Sci. Rev.*, 2023, **10**, nwac170.
11 M. T. Chorsi, E. J. Curry, H. T. Chorsi, R. Das, J. Baroody, P. K. Purohit, H. Ilies and T. D. Nguyen, *Adv. Mater.*, 2019, **31**, 1802084.
12 H. Ryu, H. J. Yoon and S. W. Kim, *Adv. Mater.*, 2019, **31**, 1802898.
13 B. Li, B. Yang, H. Zhang, J. Zhang, Q. Wang and W. Liu, *J. Materiomics*, 2024, **10**, 624–631.
14 E. Fukada, *IEEE Trans. Ultrason. Ferroelectr. Freq. Control*, 2000, **47**, 1277–1290.
15 X. Qian, X. Chen, L. Zhu and Q. M. Zhang, *Science*, 2023, **380**, eadg0902.
16 X. Chen, H. Qin, X. Qian, W. Zhu, B. Li, B. Zhang, W. Lu, R. Li, S. Zhang and L. Zhu, *Science*, 2022, **375**, 1418–1422.
17 H. S. Nalwa, *Ferroelectric polymers: chemistry: physics, and applications*, CRC Press, 1995.
18 Y. Liu, T. Yang, B. Zhang, T. Williams, Y.-T. Lin, L. Li, Y. Zhou, W. Lu, S. H. Kim, L.-Q. Chen, J. Bernholc and Q. Wang, *Adv. Mater.*, 2020, **32**, 2005431.
19 C. Liu, F. Wang and X. Du, Self-powered electrostatic tweezer for adaptive object manipulation, *Device*, 2024, **2**, 100465.
20 X. Chen, X. Han and Q.-D. Shen, *Adv. Electron. Mater.*, 2017, **3**, 1600460.
21 Y. Liu, H. Aziguli, B. Zhang, W. Xu, W. Lu, J. Bernholc and Q. Wang, *Nature*, 2018, **562**, 96–100.
22 Y. Wu, J. K. Yim, J. Liang, Z. Shao, M. Qi, J. Zhong, Z. Luo, X. Yan, M. Zhang and X. Wang, *Sci. Rob.*, 2019, **4**, eaax1594.
23 Y. Liu, Y. Zhou, H. Qin, T. Yang, X. Chen, L. Li, Z. Han, K. Wang, B. Zhang, W. Lu, L.-Q. Chen, J. Bernholc and Q. Wang, *Nat. Mater.*, 2023, **22**, 873–879.
24 K. Tashiro and H. Tadokoro, *Macromolecules*, 1983, **16**, 961–965.
25 G. Xia, J. Fang, D. Shou and X. Wang, *Prog. Mater. Sci.*, 2024, **146**, 101340.
26 B. Li, C. Cai, Y. Liu, F. Wang, B. Yang, Q. Li, P. Zhang, B. Deng, P. Hou and W. Liu, *Nat. Commun.*, 2023, **14**, 4000.
27 Y. Chen, X. Zhang and C. Lu, *Chem. Sci.*, 2024, **15**, 16436–16466.
28 C. Cai, H. Zhang, B. Li, Z. Han, F. Wang, P. Hou and W. Liu, *Adv. Electron. Mater.*, 2023, **9**, 2201084.
29 L. Gao, B.-L. Hu, L. Wang, J. Cao, R. He, F. Zhang, Z. Wang, W. Xue, H. Yang and R.-W. Li, *Science*, 2023, **381**, 540–544.
30 Q. Wang, C. R. Bowen, W. Lei, H. Zhang, B. Xie, S. Qiu, M.-Y. Li and S. Jiang, *J. Mater. Chem. A*, 2018, **6**, 5040–5051.
31 M. Ma, Z. Zhang, Z. Zhao, Q. Liao, Z. Kang, F. Gao, X. Zhao and Y. Zhang, *Nano Energy*, 2019, **66**, 104105.
32 J. Yan, M. Liu, Y. G. Jeong, W. Kang, L. Li, Y. Zhao, N. Deng, B. Cheng and G. Yang, *Nano Energy*, 2019, **56**, 662–692.
33 R. A. Surmenev, R. V. Chernozem, I. O. Pariy and M. A. Surmeneva, *Nano Energy*, 2021, **79**, 105442.
34 F. Mokhtari, A. Samadi, A. O. Rashed, X. Li, J. M. Razal, L. X. Kong, R. J. Varley and S. F. Zhao, *Prog. Mater. Sci.*, 2025, **148**, 101376.
35 J.-H. Lee, K. Y. Lee, M. K. Gupta, Y. T. Kim, D.-Y. Lee, J. Oh, C. Ryu, W. J. Yoo, C.-Y. Kang, S.-J. Yoon, J.-B. Yoo and S.-W. Kim, *Adv. Mater.*, 2014, **26**, 765–769.
36 Y.-E. Shin, S.-D. Sohn, H. Han, Y. Park, H.-J. Shin and H. Ko, *Nano Energy*, 2020, **72**, 104671.
37 A. Mubarak, B. Sarsembayev, Y. Serik, A. Onabek, Z. Kappassov, Z. Bakenov, K. Tsuchiya and G. Kalimuldina, *Energy Environ. Mater.*, 2025, **8**, e12808.
38 M. Han, H. Wang, Y. Yang, C. Liang, W. Bai, Z. Yan, H. Li, Y. Xue, X. Wang, B. Akar, H. Zhao, H. Luan, J. Lim, I. Kandela, G. A. Ameer, Y. Zhang, Y. Huang and J. A. Rogers, *Nat. Electron.*, 2019, **2**, 26–35.
39 A. Huang, Y. Zhu, S. Peng, B. Tan and X. Peng, *ACS Nano*, 2024, **18**, 691–702.
40 Y.-E. Shin, Y.-J. Park, S. K. Ghosh, Y. Lee, J. Park and H. Ko, *Adv. Sci.*, 2022, **9**, 2105423.
41 C. Wan and C. R. Bowen, *J. Mater. Chem. A*, 2017, **5**, 3091–3128.
42 A. Bindhu, A. P. Arun and M. Pathak, *ACS Appl. Electron. Mater.*, 2024, **6**, 47–72.
43 T. Bhatta, P. Maharjan, H. Cho, C. Park, S. H. Yoon, S. Sharma, M. Salauddin, M. T. Rahman, S. M. S. Rana and J. Y. Park, *Nano Energy*, 2021, **81**, 105670.
44 X. Huang and X. Zhang, *Adv. Mater. Technol.*, 2023, **8**, 2301226.
45 A. Sharma, M. Z. Ansari and C. Cho, *Sens. Actuators, A*, 2022, **347**, 113934.
46 Z. D. Sun, M. L. Zhu, Z. X. Zhang, Z. C. Chen, Q. F. Shi, X. C. Shan, R. C. H. Yeow and C. K. Lee, *Adv. Sci.*, 2021, **8**, 2100230.
47 W. Gong, W. Yang, F. Fu, X. Liu, J. Wang, X.-Q. Wang, C. Hou, Z. Wang, M. D. Dickey and H. Wang, *Nano Energy*, 2024, **131**, 110277.
48 M. Airam, F. Kargaran, A. Sabbagh, S. Ahmadi, E. A. Dawi and H. A. Khonakdar, *J. Mater. Sci.*, 2025, **60**, 63–97.
49 Y. Yang, H. Pan, G. Xie, Y. Jiang, C. Chen, Y. Su, Y. Wang and H. Tai, *Sens. Actuators, A*, 2020, **301**, 111789.
50 D. Zabek, K. Seunarine, C. Spacie and C. Bowen, *ACS Appl. Mater. Interfaces*, 2017, **9**, 9161–9167.
51 D. Zabek, J. Taylor, E. L. Boulbar and C. R. Bowen, *Adv. Energy Mater.*, 2015, **5**, 1401891.
52 J. S. Lee, G. H. Kim, S. M. Hong, H. J. Choi and Y. Seo, *ACS Appl. Mater. Interfaces*, 2009, **1**, 2902–2908.

53 L. Sarkar, S. G. Singh and S. R. Krishna Vanjari, *Smart Mater. Struct.*, 2021, **30**, 075013.
54 S. K. Karan, R. Bera, S. Paria, A. K. Das, S. Maiti, A. Maitra and B. B. Khatua, *Adv. Energy Mater.*, 2016, **6**, 1601016.
55 M.-H. You, X.-X. Wang, X. Yan, J. Zhang, W.-Z. Song, M. Yu, Z.-Y. Fan, S. Ramakrishna and Y.-Z. Long, *J. Mater. Chem. A*, 2018, **6**, 3500–3509.
56 K. Maity and D. Mandal, *ACS Appl. Mater. Interfaces*, 2018, **10**, 18257–18269.
57 A. Simaite, B. Tondu, P. Souères and C. Bergaud, *ACS Appl. Mater. Interfaces*, 2015, **7**, 19966–19977.
58 X. Hu, X. Yan, L. Gong, F. Wang, Y. Xu, L. Feng, D. Zhang and Y. Jiang, *ACS Appl. Mater. Interfaces*, 2019, **11**, 7379–7386.
59 N. Shehata, R. Nair, R. Boualayan, I. Kandas, A. Masrani, E. Elnabawy, N. Omran, M. Gamal and A. H. Hassanin, *Sci. Rep.*, 2022, **12**, 8335.
60 R. Ram, V. Soni and D. Khastgir, *Composites, Part B*, 2020, **185**, 107748.
61 Z.-H. Shen, T.-X. Tang, J. Wang, M.-J. Zhou, H.-X. Liu, L.-Q. Chen, Y. Shen and C.-W. Nan, *Nano Energy*, 2023, **117**, 108933.
62 J. Xia, H. Lu, G. Chen, D. Lin, W. Yang, C. Liu, B. Hu and Y. Zhao, *Nano Energy*, 2024, **128**, 109901.
63 J. W. Stewart, J. H. Vella, W. Li, S. Fan and M. H. Mikkelsen, *Nat. Mater.*, 2020, **19**, 158–162.
64 H. Lu, J. Zhang, L. Yang, Y. Zhang, Y. Wu and H. Zheng, *ACS Appl. Mater. Interfaces*, 2022, **14**, 12243–12256.
65 T. Tang, Z. Shen, J. Wang, S. Xu, J. Jiang, J. Chang, M. Guo, Y. Fan, Y. Xiao, Z. Dong, H. Huang, X. Li, Y. Zhang, D. Wang, L.-Q. Chen, K. Wang, S. Zhang, C.-W. Nan and Y. Shen, *Natl. Sci. Rev.*, 2023, **10**, nwad177.
66 C. Wang, X. Gao, M. Zheng, M. Zhu and Y. Hou, *ACS Appl. Mater. Interfaces*, 2021, **13**, 41735–41743.
67 K. Shi, B. Chai, H. Zou, P. Shen, B. Sun, P. Jiang, Z. Shi and X. Huang, *Nano Energy*, 2021, **80**, 105515.
68 H. Li, H. B. Lee, J.-W. Kang and S. Lim, *Nano Energy*, 2023, **113**, 108576.
69 M. N. Islam, R. H. Rupom, P. R. Adhikari, Z. Demchuk, I. Popov, A. P. Sokolov, H. F. Wu, R. C. Advincula, N. Dahotre, Y. Jiang and W. Choi, *Adv. Funct. Mater.*, 2023, **33**, 2302946.
70 F. Wang, M. Liu, C. Liu, Q. Zhao, T. Wang, Z. Wang and X. Du, *Sci. Adv.*, 2022, **8**, eabp9369.
71 F. Wang, M. Liu, C. Liu, C. Huang, L. Zhang, A. Cui, Z. Hu and X. Du, *Natl. Sci. Rev.*, 2023, **10**, nwac164.
72 F. Wang, C. Liu, Z. Dai, W. Xu, X. Ma, Y. Gao, X. Ge, W. Zheng and X. Du, *Innovation*, 2024, **6**, 100742.
73 M.-D. Li, X.-Q. Shen, X. Chen, J.-M. Gan, F. Wang, J. Li, X.-L. Wang and Q.-D. Shen, *Nat. Commun.*, 2022, **13**, 5849.
74 N. Soin, D. Boyer, K. Prashanthi, S. Sharma, A. A. Narasimulu, J. Luo, T. H. Shah, E. Siores and T. Thundat, *Chem. Commun.*, 2015, **51**, 8257–8260.
75 H. Zhou, Y. Zhang, Y. Qiu, H. Wu, W. Qin, Y. Liao, Q. Yu and H. Cheng, *Biosens. Bioelectron.*, 2020, **168**, 112569.
76 S. Lee, D. Kim, S. Lee, Y.-I. Kim, S. Kum, S.-W. Kim, Y. Kim, S. Ryu and M. Kim, *Small*, 2022, **18**, 2105811.
77 J.-H. Lee, H.-J. Yoon, T. Y. Kim, M. K. Gupta, J. H. Lee, W. Seung, H. Ryu and S.-W. Kim, *Adv. Funct. Mater.*, 2015, **25**, 3203–3209.
78 X. Chen, X. Li, J. Shao, N. An, H. Tian, C. Wang, T. Han, L. Wang and B. Lu, *Small*, 2017, **13**, 1604245.
79 V. Cauda, S. Stassi, K. Bejtka and G. Canavese, *ACS Appl. Mater. Interfaces*, 2013, **5**, 6430–6437.
80 C. Hou, W. Zhang, X. Dai, J. Qiu, T. P. Russell, X. Sun and S. Yan, *Small*, 2022, **18**, 2205790.
81 M.-C. García-Gutiérrez, A. Linares, J. J. Hernández, D. R. Rueda, T. A. Ezquerra, P. Poza and R. J. Davies, *Nano Lett.*, 2010, **10**, 1472–1476.
82 X. Chen, H. Tian, X. Li, J. Shao, Y. Ding, N. An and Y. Zhou, *Nanoscale*, 2015, **7**, 11536–11544.
83 X. Liu, Y. Shang, J. Zhang and C. Zhang, *ACS Appl. Mater. Interfaces*, 2021, **13**, 14334–14341.
84 Y. Yuan, H. Chen, H. Xu, Y. Jin, G. Chen, W. Zheng, W. Wang, Y. Wang and L. Gao, *Sens. Actuators, A*, 2022, **345**, 113818.
85 L. Song, R. Dai, Y. Li, Q. Wang and C. Zhang, *ACS Sustainable Chem. Eng.*, 2021, **9**, 7561–7568.
86 X. Guan, B. Xu and J. Gong, *Nano Energy*, 2020, **70**, 104516.
87 T. Yang, H. Pan, G. Tian, B. Zhang, D. Xiong, Y. Gao, C. Yan, X. Chu, N. Chen, S. Zhong, L. Zhang, W. Deng and W. Yang, *Nano Energy*, 2020, **72**, 104706.
88 H. Wang, H. Lin, S. Huang, L. Li, Y. Zhao and W. Zhang, *Composites, Part B*, 2024, **287**, 111841.
89 K. Roy, S. K. Ghosh, A. Sultana, S. Garain, M. Xie, C. R. Bowen, K. Henkel, D. Schmeiβer and D. Mandal, *ACS Appl. Nano Mater.*, 2019, **2**, 2013–2025.
90 B. Lu, L. Xie, H. Lei, Y. Liu, C. Zhao, X. Sun and Z. Wen, *Adv. Mater. Technol.*, 2024, **9**, 2301480.
91 B. Chai, K. Shi, Y. Wang, Y. Liu, F. Liu, L. Zhu and X. Huang, *ACS Nano*, 2024, **18**, 25216–25225.
92 A. Šutka, K. Mālnieks, A. Linarts, M. Timusk, V. Jurķāns, I. Gorņevs, J. Blūms, A. Bērziņa, U. Joost and M. Knite, *Energy Environ. Sci.*, 2018, **11**, 1437–1443.
93 G. Tian, W. L. Deng, Y. Y. Gao, D. Xiong, C. Yan, X. B. He, T. Yang, L. Jin, X. Chu, H. T. Zhang, W. Yan and W. Q. Yang, *Nano Energy*, 2019, **59**, 574–581.
94 Y. C. Guo, H. A. Zhang, L. Fang, Z. X. Wang, W. He, S. W. Shi, R. Y. Zhang, J. Cheng and P. H. Wang, *Nano Energy*, 2024, **123**, 109427.
95 Y. Li, M. Z. Qin, Q. H. Lin, J. W. Liu, S. X. Wu, Z. Yao, Y. Y. Li, T. Sun and H. Kan, *Nano Energy*, 2024, **125**, 109515.
96 M. Kazemzadeh, I. Mehdipour, M. De Vittorio and F. Pisanello, *Adv. Intell. Syst.*, 2024, **6**, 2300457.
97 F. Mokhtari, Z. Cheng, R. Raad, J. Xi and J. Foroughi, *J. Mater. Chem. A*, 2020, **8**, 9496–9522.
98 W. Zhang, C. Y. Hou, Y. G. Li, Q. H. Zhang and H. Z. Wang, *Nanoscale*, 2017, **9**, 17821–17828.
99 W. Z. Guo, C. X. Tan, K. M. Shi, J. W. Li, X. X. Wang, B. Sun, X. Y. Huang, Y. Z. Long and P. K. Jiang, *Nanoscale*, 2018, **10**, 17751–17760.

100 Y. J. Su, C. X. Chen, H. Pan, Y. Yang, G. R. Chen, X. Zhao, W. X. Li, Q. C. Gong, G. Z. Xie, Y. H. Zhou, S. L. Zhang, H. L. Tai, Y. D. Jiang and J. Chen, *Adv. Funct. Mater.*, 2021, **31**, 2010962.
101 Z. Q. Ma, W. B. Jia, J. Zhang, X. D. He, S. Y. Liu, M. E. Hilal, X. Zhou, Z. B. Yang, Z. G. Chen, P. Shi and B. L. Khoo, *Adv. Funct. Mater.*, 2024, **34**, 2470285.
102 S. Lim, D. Son, J. Kim, Y. B. Lee, J.-K. Song, S. Choi, D. J. Lee, J. H. Kim, M. Lee, T. Hyeon and D.-H. Kim, *Adv. Funct. Mater.*, 2015, **25**, 375–383.
103 B. Rostamian, M. Koolani, P. Abdollahzade, M. Lankarany, E. Falotico, M. Amiri and N. V. Thakor, *Sci. Rep.*, 2022, **12**, 21690.
104 S. Xu, J.-X. Yu, H. Guo, S. Tian, Y. Long, J. Yang and L. Zhang, *Nat. Commun.*, 2023, **14**, 219.
105 M. Zhu, T. He and C. Lee, *Appl. Phys. Rev.*, 2020, **7**, 031305.
106 S. Liu, W. M. Qing, D. Zhang, C. Z. Gan, J. C. Zhang, S. H. Liao, K. X. Wei and H. X. Zou, *Nano Energy*, 2024, **128**, 109849.
107 W. L. Deng, T. Yang, L. Jin, C. Yan, H. C. Huang, X. Chu, Z. X. Wang, D. Xiong, G. Tian, Y. Y. Gao, H. T. Zhang and W. Q. Yang, *Nano Energy*, 2019, **55**, 516–525.
108 J. W. Fastier-Wooller, T.-H. Vu, H. Nguyen, H.-Q. Nguyen, M. Rybachuk, Y. Zhu, D. V. Dao and V. T. Dau, *ACS Appl. Mater. Interfaces*, 2022, **14**, 27317–27327.
109 M. H. Syu, Y. J. Guan, W. C. Lo and Y. K. Fuh, *Nano Energy*, 2020, **76**, 105029.
110 X. Cao, Y. Xiong, J. Sun, X. Zhu, Q. Sun and Z. L. Wang, *Adv. Funct. Mater.*, 2021, **31**, 2102983.
111 H. Q. Huynh, T. Q. Trung, A. Bag, T. D. Do, M. J. Sultan, M. Kim and N.-E. Lee, *Adv. Funct. Mater.*, 2023, **33**, 2303535.
112 F. Q. Chen, Y. H. Wu, Z. Y. Ding, X. Xia, S. H. Li, H. W. Zheng, C. L. Diao, G. T. Yue and Y. L. Zi, *Nano Energy*, 2019, **56**, 241–251.
113 Y. H. Jung, S. K. Hong, H. S. Wang, J. H. Han, T. X. Pham, H. Park, J. Kim, S. Kang, C. D. Yoo and K. J. Lee, *Adv. Mater.*, 2020, **32**, 1904020.